AIAA 81-0429R

Numerical Techniques for Solving Nonlinear Instability Problems in Solid Rocket Motors

Joseph D. Baum*
University of Dayton, Dayton, Ohio
and
Jay N. Levine†
Air Force Rocket Propulsion Laboratory, Edwards Air Force Base, Calif.

The results of an investigation to select a satisfactory numerical method for calculating the propagation of steep-fronted, shock-like waveforms in a solid rocket motor combustion chamber are presented. A number of different numerical schemes were evaluated by comparing the results obtained for three related but simpler problems: the shock-tube problem, the linear wave equation, and nonlinear wave propagation in a closed tube. The most promising method, a combination of the Lax-Wendroff, Hybrid, and Artificial Compression techniques, was incorporated into an existing nonlinear combustion instability program. The capability of the modified program to treat steep-fronted wave instabilities in low-smoke tactical motors was verified by solving a number of motor test cases with disturbance amplitudes as high as 80% of the mean pressure.

Nomenclature

A = cross-section area
a = gas-only, sound speed
C_n = Courant number
c_p = specific heat of gas at constant pressure
c_s = specific heat of solid propellant
c_v = specific heat of gas at constant volume
m = mass flux from burning surface
P = pressure
T = temperature
T_f = flame temperature of the propellant
T_s = temperature at the propellant surface
T_∞ = back-wall temperature of the propellant
t = time
u = velocity
u_s = velocity of the combustion products as they enter the main flow
x = axial distance
γ = gas-only isentropic exponent
ρ = density
ω = mass burning rate, per unit length, per unit cross-sectional area

Subscript

s = burning surface

Introduction

TACTICAL solid rocket motors are frequently subject to a combustion instability problem at some point in the design cycle. When instability is encountered it can take one of several forms, such as linear or nonlinear, longitudinal or tangential. Over the last 20 years, considerable resources have been expended to understand, predict, control, and eliminate combustion instability in solid rocket motors. Most of this effort has been devoted to linear instability problems, and as a result, such problems can now be treated in a rational, cost-effective manner. Comparatively little work has been accomplished toward the understanding and resolution of nonlinear combustion instability problems. Thus, when nonlinear instabilities are encountered, the solution is too often an expensive cut-and-try process.

Linear instabilities are characterized by small-amplitude, sinusoidal oscillations that originate from the amplification of infinitesimal random disturbances in the motor chamber. On the other hand, nonlinear instabilities are usually characterized by large-amplitude oscillations having steep-fronted, shock-like waveforms. Nonlinear instability is initiated by random finite-amplitude events, such as the expulsion of an igniter or insulation fragment through the nozzle. Nonlinear instability has been modeled using both "exact" and "approximate" mathematical techniques. The "exact" methods (e.g., Refs. 1 and 2) seek to numerically solve the nonlinear partial differential equations governing both the mean and time-dependent flow in the combustion chamber, as well as the combustion response of the solid propellant. The "approximate" methods (e.g., Refs. 3 and 4) utilize perturbation techniques and harmonic analysis to reduce the problem to the solution of ordinary differential equations. The objective of the present research is to extend and improve the "exact" model developed in Ref. 1.

The existing "exact" nonlinear instability programs were developed about seven years ago and are not capable of treating the multiple-shock, steep-fronted type of instabilities that occur in variable-cross-sectional-area reduced and minimum-smoke tactical motors developed since then. The first phase of the research, the results of which are reported herein, was devoted to improving the finite-difference numerical technique used to solve the hyperbolic partial differential equations that govern wave propagation in solid rocket combustion chambers.

In order to be acceptable for the intended application, a finite difference technique must preserve the high-frequency content of the waveforms, be relatively nondissipative and nondispersive after many wave cycles, be capable of describing a shock wave as a sharp discontinuity without generating overshoots or undershoots upon crossing the discontinuity, and be capable of properly treating the reflection of shock waves from boundaries and the partial reflection and transmission at area discontinuities. It should be pointed out that, in solving a combustion instability problem, numerically induced pre- and post-shock "wiggles" do not just impair the accuracy of the solution but could also

Presented as Paper 81-0429 at the 19th Aerospace Sciences Meeting, St. Louis, Mo., Jan. 12-15, 1981; submitted Feb. 23, 1981; revision received Nov. 13, 1981. This paper is declared a work of the U. S. Government and therefore is in the public domain.

*Research Scientist; currently with the Air Force Rocket Propulsion Laboratory, Edwards A.F.B. California. Member AIAA.
†Research Physical Scientist.

falsely "trigger" nonlinear instabilities and force the scheme to pick a nonphysical solution.

It is very difficult for any single finite difference scheme to satisfy all of the aforementioned requirements simultaneously. For example, several artificial viscosity schemes[5] have been developed to damp pre- and post-shock oscillations. Such artificially introduced diffusion also smears out the discontinuity and eventually damps the high-frequency content of the waveform. Moreover, such artificial damping can be comparable in magnitude to the usual net gains or losses of acoustic energy in rocket motors; hence, its presence would seriously limit the validity of the results. In addition, use of artificial viscosity would hamper efforts to determine the actual damping of gas-phase oscillations in metallized solid-propellant rocket motors. In this connection, it should be pointed out that shock-fitting schemes[6] that treat the shock as an internal boundary are impractical for this application because of the large number of shocks traveling, interacting, and reflecting inside variable-cross-sectional-area motors. Finite difference schemes, such as the λ-scheme[7] and the split-coefficient method,[8] that are modeled after and exploit the mathematical theory of the method of characteristics are best used in conjunction with shock-fitting schemes.[9] These methods do not accurately reproduce shock location and jump conditions when used for shock capturing, even for a steady-state problem.[8] Shock-capturing implicit difference schemes offer no particular advantage for the present problem, since the physical problem of interest requires time resolution consistent with the stability restrictions of explicit methods.

In view of the deficiencies of the "older" methods —e.g., MacCormack,[10] Lax and Wendroff,[11] and Godunov[12]—several special schemes designed to achieve shock resolution without oscillations were developed. Among them are the Flux-Corrected-Transport-Pheonical schemes of Boris and Book,[13,14] Chorin's implementation of Glimm's method,[15] the upstream-centered scheme of Van Leer,[16] the second-order Godunov scheme of Van Leer,[17] the hybrid scheme of Harten and Zwas,[18] and the Artificial Compression scheme of Harten.[19] All these schemes are fixed-grid finite difference approximations to the derivatives arising in the conservation laws and can automatically handle interactions between waves of different families. In order to evaluate the suitability of the aforementioned techniques for the present purpose, their ability to treat a number of simpler, but related problems was examined. The results of this investigation are summarized in the next section. The finite difference scheme judged most promising was then incorporated into the nonlinear combustion instability program described in Ref. 1. The results of a number of nonlinear combustion instability solutions are presented to demonstrate the effectiveness of the new technique.

Test Problem Results

As a first step in evaluating the various finite difference schemes (the algorithms for these schemes were omitted due to lack of space), they were utilized to solve the shock-tube problem for the one-dimensional Eulerian form of the gas-dynamic conservation equations for an inviscid, non-heat-conducting fluid. (Results of a similar investigation were reported by Sod.[20]) These solutions were utilized to rate the difference schemes based upon such criteria as resolution of the shock (i.e., number of mesh points needed to describe the shock discontinuity), diffusion and smearing of the shock and the contact discontinuities with time, stability, effect of Courant number, and computation time.

The results of the shock-tube test case demonstrated the superiority of the recently developed techniques[13-19] over earlier methods.[10-12] The advanced methods require only approximately 20% more storage and computation time than the standard methods. Very good results were produced by the Flux-Corrected Transport-Shasta schemes.[13,14] Nevertheless, based on the previously mentioned criteria, the best method was a combination of the basic Lax-Wendroff scheme,[11] with the Hybrid scheme,[18] and the Artificial Compression method[19] (LW + H + ACM). This method involves two steps; in the first step, the second-order Lax-Wendroff scheme is hybridized with a nonoscillatory first-order-accurate method to allow a monotonic (i.e., nonoscillatory) transition of discontinuities; in the second step, artificial compression is applied to sharpen transitions of discontinuities since the hybridized first-order-accurate method is too dissipative. A switch value that is based upon flow gradients (density has been used in this research work) is utilized to activate the artificial compression and the first-order monotonic scheme in regions of admissible discontinuities only. This combined method preserves the second-order truncation error of the Lax-Wendroff scheme and yet yields a sharp and oscillation-free transition of both shocks and contact discontinuities. The combined scheme is too long to be included here. Details are given in Refs. 18 and 19.

The various finite difference methods were also employed to solve the test problem of a one-dimensional linear standing wave in a tube. The results were used to evaluate the relative diffusive and dispersive errors of the schemes for harmonic standing wave propagation after many wave cycles. This problem was also used to assess the ease of implementation of boundary conditions for the techniques considered.

The linear wave equation solutions demonstrated the dependence of the diffusive and dispersive errors upon Courant number and spatial step size. In addition, it has been demonstrated that the magnitude of the diffusive and dispersive errors varies significantly from one method to another. The LW + H + ACM combination method and the Flux-Corrected-Transport-Pheonical schemes[13,14] produced excellent solutions to this problem, with little error evident after many wave cycles.

The final test leading to selection of a method to be utilized in the nonlinear instability program was the solution of the one-dimensional, nonlinear hyperbolic equations describing finite-amplitude wave and shock propagation in a closed-end tube. By establishing different initial conditions, it was possible to compare results obtained with the various techniques for problems ranging from almost linear (small initial disturbances) to highly nonlinear (large disturbances and shocks) conditions, over a large number of wave cycles. Results obtained with these techniques for problems such as interactions of different wave families and the effect of change in grid size and Courant number upon the waveform and the frequency content of the results were compared. Some of these results are presented to illustrate differences between the numerical techniques. In this connection, it should be mentioned that, owing to the large variations of the mean flow inside a rocket motor, one has to deal with Courant numbers varying from 0.3 to close to unity. The solutions presented herein were obtained with a Courant number of 0.6. Other solutions were obtained at higher and lower Courant numbers to confirm that the conclusions regarding the relative merits of each scheme were valid in general.

As a result of the numerical errors associated with finite difference methods, each technique acts as a numerical filter. The "filtering" effect of each of the techniques is a different function of frequency, mesh size, etc. To enhance the ability to discern these differences, the results of the test problems were spectrally analyzed.

Figures 1, 2, and 4 demonstrate the effect of numerical technique on the time evolution of acoustic pressure amplitude at an end of a closed tube. The solutions were initiated utilizing a first-harmonic standing wave perturbation having an amplitude of 20% of the mean pressure. The numerical schemes used in the figures were the LW + H + ACM method (Fig. 1), the MacCormack scheme[10] (Fig. 2), the Flux-Corrected Transport-Shasta-Pheonical-Lax-Wendroff[13] (Fig. 4a), and the Flux-Corrected-Transport-Shasta-Pheonical

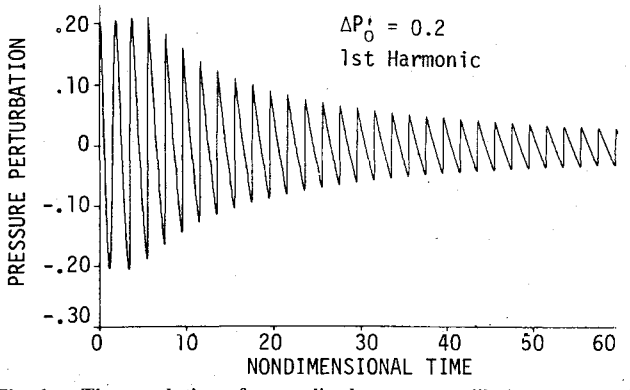

Fig. 1a Time evolution of normalized pressure oscillations at an end of a tube (Lax-Wendroff + hybrid + ACM scheme).

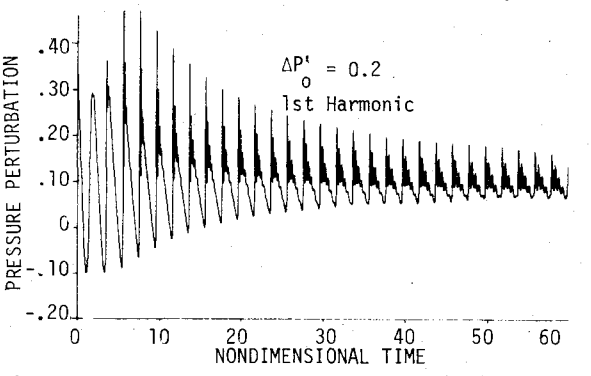

Fig. 2a Time evolution of normalized pressure oscillations at an end of the tube (MacCormack).

Fig. 1b Expanded view of normalized pressure oscillations at an end of the tube (LW + H + ACM).

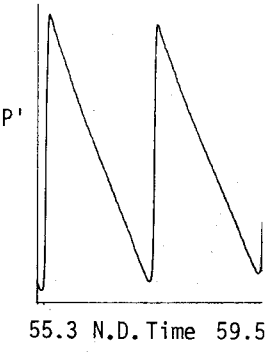

Fig. 1c Power spectral density as a function of frequency (LW + H + ACM).

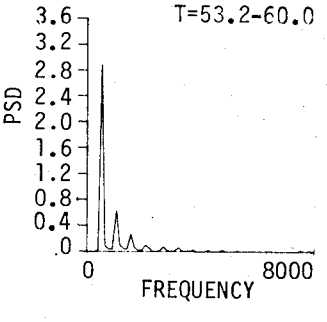

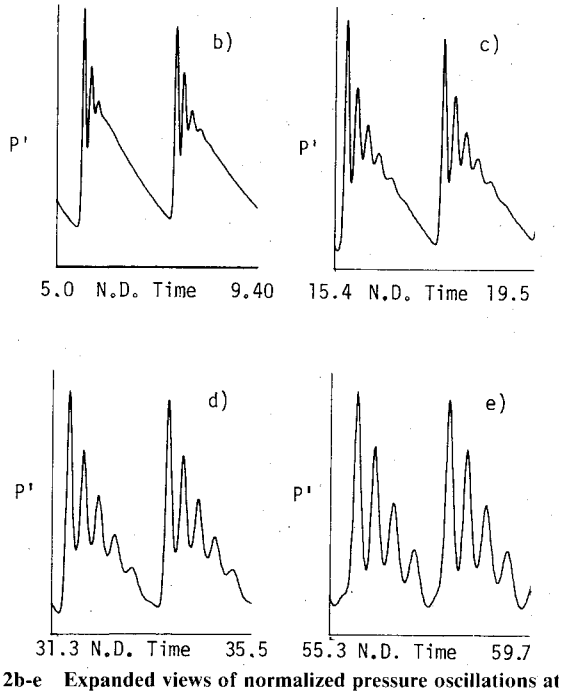

Figs. 2b-e Expanded views of normalized pressure oscillations at an end of the tube (MacCormack).

Low-Phase Error[14] (Fig. 4b). Spectral analyses of the results shown in Figs. 1b and 2 are presented in Figs. 1c and 3, respectively.

Figure 1a shows the time evolution of the normalized pressure oscillations at an end of the tube as obtained with the LW + H + ACM technique. The initial sine wave disturbance develops into a sharp, triangular, shock-type waveform. This is the expected result based on the closed-form analytical solution to this problem, e.g., Ref. 21. The decay in shock amplitude observed in Fig. 1a is not a result of numerical dissipation, but rather a result of entropy increase due to repetitive shock wave processing of the gas in the tube. The rate of decay corresponds to the theoretically calculated decay rate.[21] Figure 1b shows an expanded view of the pressure waveform for the nondimensional time period of 55.3 and 59.5. The shocks shown in this figure have sharp resolution (the shock is captured over three mesh points = 2 zones) and are oscillation-free. Figure 1c presents the power spectral density as a function of frequency for this time interval. The spectral analysis of the N-wave analytical solution for this problem can be obtained in a closed form. The solution for this problem indicates that the ratio of energy contained at the nth harmonic to energy contained at the first harmonic goes down as $1/n^2$. Spectral analysis of the results (at any time period) indicates excellent agreement with the analytical solution. The numerical results contain frequencies up to the 25th harmonic, which is the highest that can be observed with the 51 spatial grid points utilized. The acoustic energy distribution among the modes varies little with time (once a shock is formed), as expected. The transfer of energy from the fundamental to the higher harmonics results from the physical process of wave steepening. There is no physical process present in this model for transferring energy the other way, i.e., from higher harmonics into the fundamental mode.

Figure 2a shows the time evolution of acoustic pressure amplitude at an end of a closed tube utilizing MacCormack's scheme. Expanded views of the acoustic pressure amplitude between nondimensional times of 5.0 and 9.4, 15.4 and 19.5, 31.3 and 35.5, and 55.3 and 59.7 are shown in Figs. 2b-e, respectively. Development of the initial post-shock wiggles into erroneous oscillations is evident. Spectral analysis of these results (shown in Figs. 3a-d) clearly shows that evolution of the initial post-shock wiggles into discrete "humps" is due to two related effects: the erroneous transfer of energy between modes, due to dispersive errors that cause pressure signals to travel at the wrong speed; and dissipative errors that result in overdamping of the high-frequency modes. Figure 3a indicates an excessively high percentage of acoustic energy in the ninth to eleventh harmonics whereas Fig. 3b indicates excessive acoustic energy in the eighth and ninth harmonics. Toward the end of the test (after about 25 wave cycles), it is shown (Fig. 3d) that the excessively high percentage of

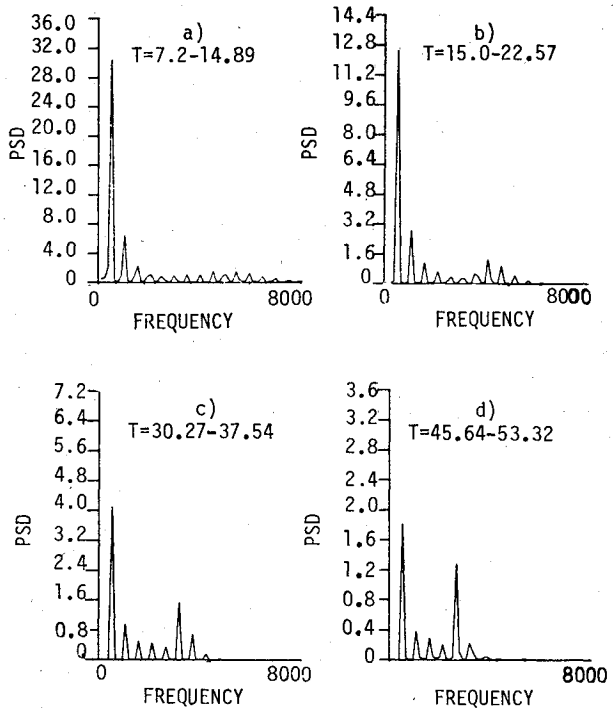

Fig. 3 Time evolution of power spectral density as a function of frequency (MacCormack).

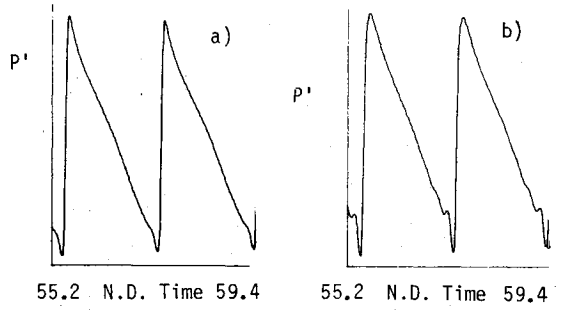

Fig. 4 Expanded view of normalized pressure oscillations at an end of the tube; a) FCT-LW; b) FCT-LPE.

acoustic energy has been transferred to the fifth and sixth harmonics. As previously mentioned, there are no known physical processes that can cause such a transition of energy from a higher to a lower mode. This fact, and the theoretical results shown in Ref. 22, support the aforementioned conclusions regarding the source of errors. The results presented in this reference (although obtained by linear analysis) indicated that, for the MacCormack scheme at $C_n = 0.6$, the dissipative errors of harmonics higher than the fourth-fifth increase with mode number. It is also shown that the dispersive errors for the high harmonics are significant at $C_n = 0.6$ and increase with a decrease in Courant number. This behavior was substantiated by additional solutions for this test case.

The results obtained utilizing the Rubin-Burstein[23] and Lax-Wendroff schemes[11] are, as expected, generally similar to the results obtained by utilizing MacCormack's scheme. The results indicate that the first post-shock wiggle appears after the third wave cycle with the Rubin-Burstein and Lax-Wendroff schemes as compared with the second wave cycle with the MacCormack scheme. Also, the percentage of energy contained in the fundamental mode is greater and the erroneously high energy in the higher modes is somewhat less with the Rubin-Burstein and Lax-Wendroff schemes.

Figure 4a shows the normalized pressure oscillations at an end of the closed tube as obtained with Book, Boris, and Hain's Flux-Corrected-Transport-Shasta-Pheonical scheme[13] as applied to the Lax-Wendroff scheme (referred to herein as FCT-LW), between the nondimensional times of 55.2 to 59.4. The shock waves shown in this figure have sharp resolution and are captured over 3 mesh points (even after 30 wave cycles). Nevertheless, both small pre- and post-shock wiggles are evident in the solution.

Figure 4b shows the pressure waveform at an end of the tube as obtained with Boris and Book's Flux-Corrected-Transport-Shasta-Pheonical Low-Phase Error scheme[14] (referred to herein as FCT-LPE) between the nondimensional times of 55.2 to 59.4. The small initial pre-shock error develops with time into a pre-shock wiggle. In addition, the shock corners become rounded with time. Nevertheless, 95% of the shock is still captured over 3 mesh points. The spectral analysis results obtained with FCT-LW and FCT-LPE are not significantly different than the results obtained with LW+H+ACM. Hence, the explanation for these imperfections in the resulting waveforms is not readily apparent.

All the earlier methods, i.e., MacCormack, Lax-Wendroff, and Rubin-Burstein, were utilized without adding artificial viscosity. The addition of an artificial viscosity term to a numerical scheme was conceived as a way to damp post-shock oscillations. Artificial viscosity does reduce post-shock oscillations, but at the expense of the higher-harmonic components of the waveform. The effect of an artificial viscosity on the solution over many wave cycles was explored using Hyman's predictor-corrector scheme (as described by Sod[20]). Results obtained utilizing this method with a high value of artificial viscosity (δ equal unity in Hyman's method) indicate that high artificial viscosity prevents a shock from ever forming and the deviations from a perfect sine wave are never large. Spectral analysis of this solution shows a complete absence of higher-harmonic content. Initially, only the first three harmonics are excited, while at a nondimensional time of 60, 99% of the energy is contained in the fundamental mode. Reducing the artificial viscosity coefficient ($\delta = 0.3$, the lowest value at which Hyman's method remains stable) yields a much steeper waveform, but one whose higher-harmonic content is still less than it should be. Initially, 15 harmonics are excited, but only the first 6 harmonics remain excited after 30 wave cycles. As time increases, the action of the artificial viscosity continues to preferentially damp the higher harmonics, causing the solution to further degenerate.

As mentioned earlier, artificial viscosity schemes would hamper efforts to determine the actual damping of gas-phase oscillations in metallized solid propellants. To illustrate the similarity between the effects of particles and artificial viscosity, the previously described closed-end tube problem was modified by the addition of 2% (particle to gas weight flow ratio) of 5-μm particles. The results obtained with the LW+H+ACM scheme are very similar to the results obtained with Hyman's scheme (with $\delta = 0.3$). With particles present, the damping of the high-frequency content of the waveform is due to a real physical process. This is in contrast to the similar, but nonphysical, action of an artificial viscosity.

Motor Solutions

The test problem solutions were used to rank the various methods according to the previously mentioned criteria. It was concluded that the Lax-Wendroff + Hybrid + Artificial Compression scheme yielded the best results. In order to demonstrate that this method retains its effectiveness when applied to the solution of actual combustion instability problems, it was incorporated into an existing nonlinear combustion instability program. This program is capable of treating general one-dimensional two-phase-flow problems in variable-area chambers and also contains a complete nonlinear transient burning rate model for solid propellants. The detailed development of this analysis is given in Ref. 1.

The quasi-one-dimensional equations of motion for gas only flow in a constant-cross-sectional-area motor can be written in conservative form as follows:

Continuity:

$$\frac{\partial \rho}{\partial t} + \frac{\partial}{\partial x}(\rho u) = \omega$$

Momentum:

$$\frac{\partial (\rho u)}{\partial t} + \frac{\partial}{\partial x}(p + \rho u^2) = 0$$

Energy:

$$\frac{\partial}{\partial t}\left[\rho\left(C_v T + \frac{u^2}{2}\right)\right] + \frac{\partial}{\partial x}\left[\rho u\left(C_p T + \frac{u^2}{2}\right)\right] = -\frac{\partial}{\partial x}(up) + \omega\left(C_p T_f + \frac{u_s^2}{2}\right)$$

The propellant properties and motor geometry [cylindrically perforated grain 0.597 m (23.5 in.) long] were taken from Ref. 1 to facilitate comparison with the earlier results. Before presenting the results of the motor solutions, it should be mentioned that, for the motor, propellant, and operating conditions utilized, a linear stability analysis shows the fundamental mode to be unstable while all the higher modes are stable. It should also be pointed out that velocity coupling effects are not included in the solutions presented herein.

Figure 5 shows the pressure/time history at the head end of the motor calculated using the LW + H + ACM scheme and an initial first-mode disturbance amplitude of 0.4 of the mean pressure. The initially sinusoidal wave is seen to transition after two wave cycles into a sharp, oscillation-free, shock-type waveform. After the nondimensional time of 20, the wave reaches a limit cycle condition with an amplitude (peak to peak) equal to 21.73% of the mean pressure. Examination of the phase differences between the pressure at different locations indicates that the solution is neither a standing wave nor a traveling wave, but is a combination of both.

To examine the effect of initial disturbance characteristics on limiting amplitude, the same problem was solved using the LW + H + ACM scheme with initial first-mode disturbance amplitudes of 0.2 and 0.05 of the mean pressure and with two different pulse-type disturbances. With all three sinusoidal initial disturbances (0.4, 0.2, and 0.05 initial amplitudes), the solution reached the same limiting amplitude; a limit cycle is reached when the gains and losses of acoustic energy equilibriate. The primary factor in achieving this equilibriation is the balance between the combustion driving and the energy transfer between modes due to the process of wave steepening. Figures 6a and 6b show the power spectra for the 0.05 initial amplitude case at nondimensional times of 0.0 to 7.5 and 45.6 to 53.26, respectively. The initial perturbation contained energy only in the fundamental mode. All of the energy observed in the higher harmonics at the later time was transferred from the fundamental mode.

An important application of nonlinear instability analyses is the prediction of motor response to pulse-type disturbances. The results of two solutions that test the ability of the LW + H + ACM scheme to treat such problems are discussed. In both cases, the initial pressure disturbance waveform was taken to be of the form $\sin^6(\pi X/L)$, producing a centered symmetric waveform with an amplitude equal to 0.4 of the mean pressure. The difference between the two cases was the initial velocity at $t=0$. In the first case, the nondimensional velocity was taken to be $\Delta P/\gamma$, whereas in the second case, the velocity was taken to be zero. The first case represents a

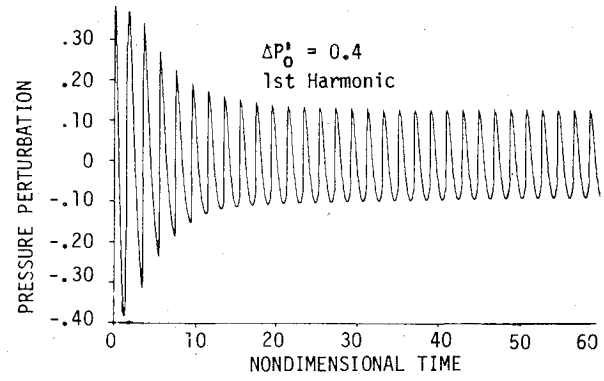

Fig. 5 Time evolution of normalized pressure oscillations at the head end of the motor (LW + H + ACM).

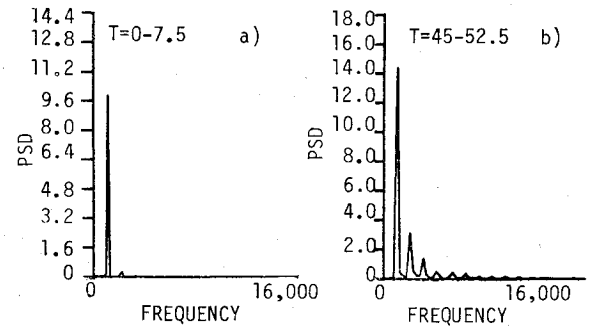

Fig. 6 Time evolution of power spectral density as a function of frequency (LW + H + ACM).

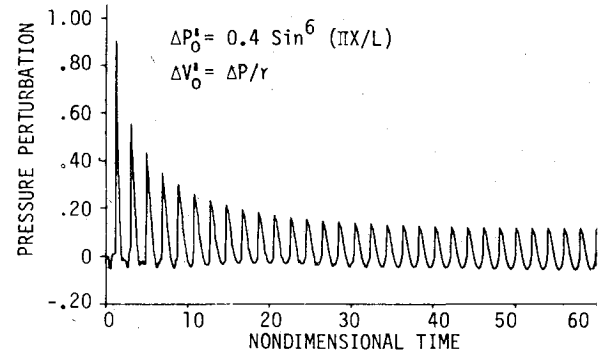

Fig. 7 Time evolution of normalized pressure oscillations at the head end of the motor for a traveling pulse (LW + H + ACM).

traveling pulse. (Actually setting $\Delta v = \Delta p/\gamma$ only produces a pure right-traveling wave in the linear limit as Δp approaches zero.) The second case corresponds to a standing pulse. The pulse propagates as the sum of equal left- and right-traveling waves, each having half the initial amplitude.

The calculated pressure histories at the head end of the motor for each of these disturbances are shown in Figs. 7 (traveling) and 8 (standing). The dramatic difference between the results demonstrates the importance of specifying the velocity disturbance associated with a pressure pulse. The traveling pulse is immediately transformed into a steep-fronted, shock-type waveform and decays until it reaches the same limiting amplitude as the solutions started from first-harmonic sinusoidal disturbances (21.73% of the mean pressure). Spectral analysis of this solution indicates that, at early times, the traveling pulse disturbance contains a large percentage of the fundamental, but a significant higher-harmonic content is also evident.

The pressure history of the standing pulse disturbance is shown in Fig. 8. The time variation of the waveform is quite

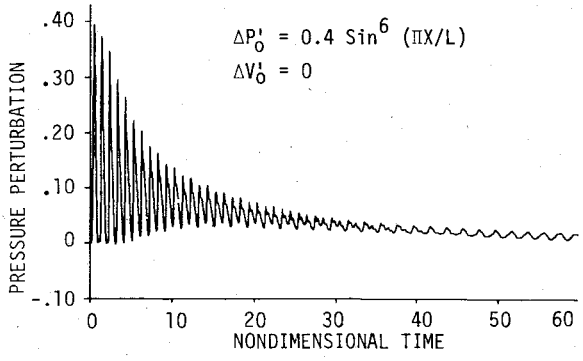

Fig. 8 Time evolution of normalized pressure oscillations at the head end of the motor for a standing pulse (LW + H + ACM).

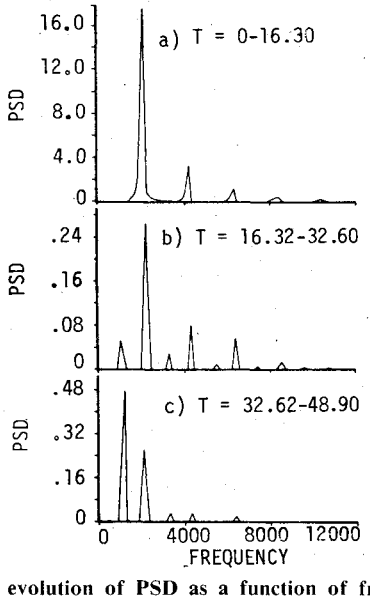

Fig. 9 Time evolution of PSD as a function of frequency for a standing pulse (LW + H + ACM).

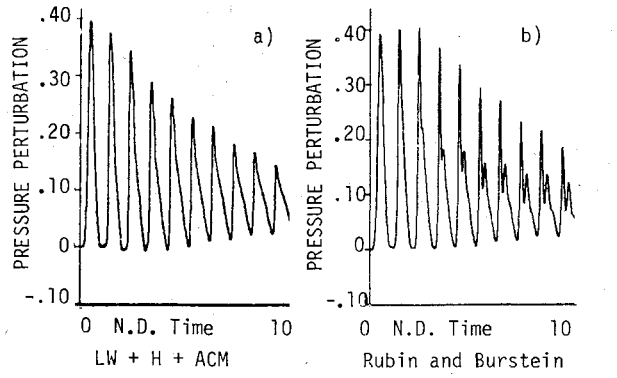

Fig. 10 Expanded views of normalized pressure oscillations at the head end of the motor for a standing pulse.

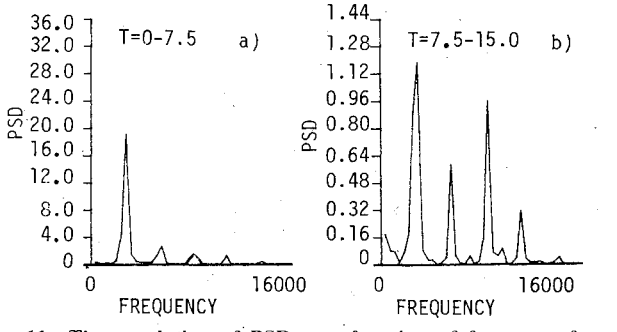

Fig. 11 Time evolution of PSD as a function of frequency for a standing pulse (Rubin-Burstein).

complex in this case. The power spectra results shown in Figs. 9a-c help to clarify what is happening. At early times, a symmetric standing pulse centered in the motor excites essentially only even harmonics (Fig. 9a), with the second harmonic dominating. The fundamental and odd harmonics are very small at this time. Since only the fundamental is unstable for this motor, the even harmonics decay with time, while the fundamental begins to grow. In the time interval from about $t = 20$ to 40, the waveform becomes complex as it transitions from a steep second-harmonic-dominated wave to an almost sinusoidal wave at the fundamental frequency. At a later time, this solution was continued out to a nondimensional time of 180. The wave continues to decay out to a time of about 100. At this time, the wave amplitude is only 1.6% of the mean pressure (compared with 40% initially) and the wave is essentially a pure fundamental sine wave. After $t = 100$, the wave starts to grow again. As the wave grows and steepens up, higher-harmonic content again begins to appear as a result of energy transfer from the fundamental to the higher harmonics, and the solution reaches the same limit cycle achieved with the other initial perturbations. Based on these results, it has been tentatively concluded that the limit cycle amplitude and waveform are independent of initial disturbance characteristics. Further studies of limiting amplitude phenomena under more general conditions will be presented in the future.

Figures 10a and 10b show the expanded views of the time evolution of the pressure oscillations for the standing pulse test case between the nondimensional times of zero and 10. Figure 10a was computed utilizing the LW + H + ACM method, whereas Fig. 10b shows the result obtained using the Rubin-Burstein scheme. The erroneous development of higher modes when utilizing the Rubin-Burstein scheme is evident after the third wave cycle. Spectral analysis of the Rubin-Burstein solution indicates that the fourth and sixth harmonics contain erroneously high energy at the nondimensional time period of 7.5 to 15 (as shown in Figs. 11a and 11b). Even in this case, in which all modes except the fundamental are stable, the effect of such erroneous higher-mode content is not merely cosmetic. When perturbed with a first-mode disturbance, the Rubin-Burstein results reached a limiting amplitude approximately 50% higher than the limiting amplitude obtained with the LW + H + ACM scheme. Such a difference can be critical when one considers the vibration levels that can be tolerated by guidance and control systems. These results conclusively demonstrate the superiority of the LW + H + ACM scheme over the generalized Lax-Wendroff-type schemes for the present class of problems.

Conclusions

Based on the results presented herein, it is concluded that the original objective of developing a method capable of solving nonlinear instability problems in smokeless tactical rocket motors has been successfully accomplished. It has been shown that all numerical methods introduce errors and that the numerical method and the physical problem to be solved need to be matched. For the present problem, a method based on the combination of the Lax-Wendroff, Hybrid, and Artificial Compression schemes was found to be superior to the other schemes tested. It has been shown that this scheme is capable of describing a shock as a sharp discontinuity without generating artificial pre- or post-shock oscillations. The method does not rely on the use of an artificial viscosity and is capable of preserving the high-frequency content of the waveforms. This combination technique can also treat the

reflection of shocks from boundaries and has small diffusive and dispersive errors even after many wave cycles.

The ability to spectrally analyze the computed results was added to the nonlinear instability program. This capability simplifies the interpretation of complex waveforms and facilitates comparisons with motor data and with the results of approximate nonlinear methods.

It has been demonstrated that, in addition to the amplitude, waveform, and location of the pressure pulse, the details of the associated velocity disturbance are also very important in determining motor response, even when velocity coupling is not considered.

The solution of an instability problem reached a limiting amplitude that was independent of the initial disturbance amplitude and waveform. The generality of this result will be the subject of future studies.

Finally, it has been shown that the use of artificial viscosity results in the nonphysical attenuation of the high harmonics. Thus, the use of a numerical method that relies on an artificial viscosity to damp post-shock oscillations is not recommended for problems that require the solution to extend over many wave cycles.

Acknowledgment

This work was partially supported under Air Force Contract F04611-81-C-0012.

References

[1] Levine, J. N. and Culick, F. E. C., "Nonlinear Analysis of Solid Rocket Combustion Instability," Air Force Rocket Propulsion Lab., TR-74-45, Oct. 1974.

[2] Kooker, D. E. and Zinn, B. T., "Numerical Solution of Axial Instabilities in Solid Propellant Rocket Motors," *10th JANNAF Combustion Meeting,* Vol. 1, Naval War College, Newport, R. I., Aug. 1973, pp. 389-416.

[3] Culick, F. E. C., "Nonlinear Behavior of Acoustic Waves in Combustion Chambers," *10th JANNAF Combustion Meeting,* Vol. 1, Naval War College, Newport, R. I., Aug. 1973, pp. 417-436; also CPIA Pub. 243, pp. 417-436.

[4] Powell, E. A., Padmanabhan, S., and Zinn, B. T., "Approximate Nonlinear Analysis of Solid Rocket Motors and T-Burners," AFRPL-TR-77-48, 1977.

[5] Lapidus, A., "A Detached Shock Calculation by Second-Order Finite Differences," *Journal of Computational Physics,* Vol. 2, 1967, pp. 154-177.

[6] Moretti, G., "The Choice of a Time-Dependent Technique in Gas Dynamics," Polytechnical Institute of Brooklyn, PIBAL Rept. 69-26, July 1969.

[7] Moretti, G., "The λ-Scheme," *Computers and Fluids,* Vol. 17, 1979, pp.191-205.

[8] Chakravarthy, S. R., Anderson, D. A., and Salas, M. D., "The Split-Coefficient Matrix Method for Hyperbolic Systems of Gas Dynamic Equations," AIAA Paper 80-0268, Jan. 1980.

[9] Marconi, F., Rudman, S., and Calia, V., "Numerical Study of One-Dimensional Unsteady Particle-Laden Flows with Shocks," *AIAA Journal,* Vol. 19, Oct. 1981, pp. 1294-1301.

[10] MacCormack, R. W., "Proceedings of the Second International Conference on Numerical Methods in Fluid Dynamics," *Lecture Notes in Physics,* edited by M. Holt, Vol. 8, Springer-Verlag, New York, 1971, pp. 151-163.

[11] Lax, P. D. and Wendroff, B., "System of Conservation Laws," *Communications on Pure and Applied Mathematics,* Vol. 13, 1960, pp. 217-237.

[12] Godunov, S. K., "Finite Difference Methods for Numerical Computations of Discontinuous Solutions of Equations of Fluid Dynamics," *Mathematics Systems,* Vol. 47, 1959, pp. 271-295.

[13] Book, D. L., Boris, J. P., and Hain, K., "Flux-Corrected Transport II: Generalization of the Method," *Journal of Computational Physics,* Vol. 18, 1975, pp. 248-283.

[14] Boris, J. P. and Book, D. L., "Flux-Corrected Transport III: Minimum Error FCT Algorithms," *Journal of Computational Physics,* Vol. 20, 1976, pp. 397-431.

[15] Chorin, A. J., "Random Choice Solution of Hyperbolic Systems," *Journal of Computational Physics,* Vol. 22, Dec. 1976, pp. 517-533.

[16] Van Leer, B., "Towards the Ultimate Conservative Difference Scheme III: Upstream-Centered Finite-Difference Scheme for Ideal Compressible Flows," *Journal of Computational Physics,* Vol. 23, March 1977, pp. 263-275.

[17] Van Leer, B., "Towards the Ultimate Conservative Difference Scheme, V: A Second-Order Sequel of Godunov's Method," *Journal of Computational Physics,* Vol. 32, 1979, pp. 101-136.

[18] Harten, A. and Zwas, G., "Self-Adjusting Hybrid Schemes for Shock Computations," *Journal of Computational Physics,* Vol. 9, 1972, pp. 568-583.

[19] Harten, A., "The Artificial Compression Method for Computation of Shocks and Contact Discontinuities: III. Self-Adjusting Hybrid Schemes," AFOSR TR-77-0659, March 1977.

[20] Sod, G. A., "A Survey of Finite Difference Methods for Systems of Nonlinear Hyperbolic Conservation Laws," *Journal of Computational Physics,* Vol. 27, 1978, pp. 1-31.

[21] Morse, P. M. and Ingard, K. V., *Theoretical Acoustics,* McGraw-Hill, New York, 1968.

[22] Warming, R. F. and Beam, M. R., "Upwind Second-Order Difference Schemes and Applications in Aerodynamic Flows," *AIAA Journal,* Vol. 14, Sept. 1976, pp. 1241-1249.

[23] Rubin, E. L. and Burstein, S. Z., "Difference Methods for the Inviscid and Viscous Equations of a Compressible Gas," *Journal of Computational Physics,* Vol. 2, 1967, pp. 178-196.